Published in Journal of Organometallic Chemistry 696, issue 3, 702–708, 2011
which should be used for any reference to this work

Study of half sandwich platinum group metal complexes containing tetradentate N-donor ligand bearing two di-pyridylamine units linked by an aromatic spacer

Gajendra Gupta [a], Sairem Gloria [a], Bruno Therrien [b], Babulal Das [c], Kollipara Mohan Rao [a,*]

[a] Department of Chemistry, North Eastern Hill University, Shillong 793022, India
[b] Service Analytique Facultaire, Université de Neuchâtel, Case Postale 158, CH-2009 Neuchâtel, Switzerland
[c] Department of Chemistry, Indian Institute of Technology, Guwahati, India

A B S T R A C T

A general approach for the preparation of dinuclear η^5- and η^6-cyclic hydrocarbon platinum group metal complexes, *viz*. $[(\eta^6\text{-arene})_2Ru_2(NN\cap NN)Cl_2]^{2+}$ (arene = C_6H_6, **1**; *p*-^{i}PrC_6H_4Me, **2**; C_6Me_6, **3**), $[(\eta^5\text{-}C_5Me_5)_2M_2(NN\cap NN)Cl_2]^{2+}$ (M = Rh, **4**; Ir, **5**), $[(\eta^5\text{-}C_5H_5)_2M_2(NN\cap NN)(PPh_3)_2]^{2+}$ (M = Ru, **6**; Os, **7**), $[(\eta^5\text{-}C_5Me_5)_2Ru_2(NN\cap NN)(PPh_3)_2]^{2+}$ (**8**) and $[(\eta^5\text{-}C_9H_7)_2Ru_2(NN\cap NN)(PPh_3)_2]^{2+}$ (**9**), bearing the bis-bidentate ligand 1,2-bis(di-2-pyridylaminomethyl)benzene (*NN*∩*NN*), which contains two chelating di-pyridylamine units connected by an aromatic spacer, is reported. The cationic dinuclear complexes have been isolated as their hexafluorophosphate or hexafluoroantimonate salts and characterized by use of a combination of NMR, IR and UV–vis spectroscopic methods and by mass spectrometry. The solid state structure of three derivatives, [**2**][SbF_6]$_2$, [**3**][PF_6]$_2$ and [**4**][PF_6]$_2$, has been determined by X-ray structure analysis.

Keywords

Arene ruthenium compounds, Cp*rhodium complexes, 1,2-Bis(di-2-pyridylaminomethyl)benzene, ligand

1. Introduction

The coordination chemistry of 2,2-di-pyridylamine (dpa) and its derivatives has been the focus of a considerable number of investigations. For example, mono-, di- and tri-dpa derivatives have been reported in which the secondary nitrogen of each dpa is directly bound to an aryl core with such species being employed in studies that range from metal coordination to supramolecular chemistry [1,2] and the synthesis of new luminescent materials [3–5]. The use of Ag(I) in a range of metal complex and supramolecular materials has received increasing attention, in part due to the coordination flexibility of this d^{10} ion and its well documented tendency to form strong complexes with nitrogen donor ligands. It is well established that upon coordination with the metal centers pyridyl rings of dpa adopt either nearly co-planar or inclined pyridyl ring planes. This property of dpa and its derivatives induces either electronically or stereo chemically in the systems and have been observed in a number of metal complexes [6,7]. Furthermore, the amine proton of dpa becomes more acidic upon complexation to the metal centre and both protonated as well as deprotonated (dpa^-) complexes based on a number of metal ions have been studied [8–10]. The loss of this proton is believed to result in a planar ligand configuration in the complexes [11]. Palladium(II) and platinum(II) complexes of both the dpa and its extended derivatives have also been investigated as potential anticancer agents due to their structural similarity to cisplatin [12–14].

Chloro-bridged dimeric arene ruthenium, rhodium and iridium complexes and monomeric arene ruthenium triphenylphosphine complexes played a vital role in organometallic chemistry [15–18]. While the reactivity of these valuable precursors with a variety of nitrogen ligands has been reported by our group [19–27], however the study with di-pyridylamine derivative containing an aromatic spacer unit such as 1,2-bis(di-2-pyridylaminomethyl)benzene (*NN*∩*NN*) has not yet been explored. This ligand has formed mononuclear, dinuclear, trinuclear and tetra-nuclear complexes with metals [28] and it also possesses the ability to form poly-pyridyl cages with silver and other metals by varying the spacer units. But surprisingly in the case of arene ruthenium and Cp* (pentamethylcyclopentadienyl) rhodium or iridium systems, it only forms dinuclear complexes despite of varying the metal ligand ratio. In this paper, we describe slight modified procedure of synthesis of the ligand which has been previously reported by Steel and coworkers [28], and the synthesis of nine novel dinuclear η^5- and η^6-cyclic hydrocarbon platinum group metal complexes bearing the ligand 1,2-bis(di-2-pyridylaminomethyl)benzene (*NN*∩*NN*) (Chart 1).

* Corresponding author.
E-mail address: mohanrao59@gmail.com (K. Mohan Rao).

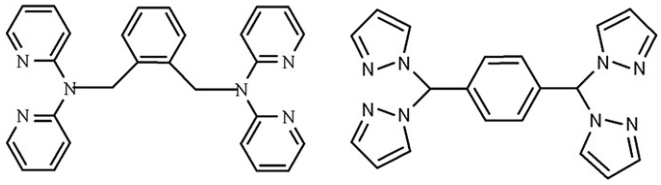

Chart 1. *NN∩NN* tetradentate ligand 1,2-bis(di-2-pyridylaminomethyl)benzene and 1,4-bis{bis(pyrazolyl-methyl)}benzene.

2. Results and discussion

The synthesis of the ligand 1,2-bis(di-2-pyridylaminomethyl) benzene (*NN∩NN*), which has been previously reported by Steel and coworkers [28], was re-examined. This new method has an advantage over the previous method as it saves considerable amount of time as compared to that of the reported procedure (2 days). The ligand structure was confirmed by proper comparison with the literature [28] and the detailed procedure is given in Experimental section.

*2.1. Dinuclear arene ruthenium, rhodium and iridium complexes **1**–**5***

The dinuclear arene ruthenium complexes $[(\eta^6\text{-arene})Ru(\mu\text{-Cl})Cl]_2$ react with the *NN∩NN* tetradentate bis(dipyridylaminomethyl) benzene ligand in methanol to afford the cationic dinuclear complexes $[(\eta^6\text{-arene})_2Ru_2(NN\cap NN)Cl_2]^{2+}$ (arene = C_6H_6, **1**; *p*-^{i}PrC_6H_4Me, **2**; C_6Me_6, **3**), isolated as their hexafluorophosphate or hexafluoroantimonate salts (Scheme 1). Compounds [**2**][SbF_6]$_2$ and [**3**][PF_6]$_2$ are yellow in color, while [**1**][PF_6]$_2$ is brown. These salts are non-hygroscopic and stable in air as well as in solution. They are sparingly soluble in polar solvents like dichloromethane, chloroform, acetone and acetonitrile but are insoluble in non-polar solvents like hexane, diethylether and petroleum ether. All compounds are characterized by ^{1}H NMR and IR spectroscopy and mass spectrometry. In the mass spectra, they show the expected molecular ion peaks *m*/*z* at 871.3, 851.4 and 1042.4, corresponding to $[\mathbf{1}]^{2+}$, $[\mathbf{2}]^{2+}$ and $[\mathbf{3}]^{2+}$ respectively. All these halogenated complexes also displayed prominent peaks corresponding to the loss of both chloride ions from the molecular ion peak $[M\text{-}(PF_6)_2]^+$, but the loss of arene group is not observed indicating the stronger bond of metal to arene group. The IR spectra of these complexes exhibit a sharp band due to chelated *NN∩NN* tetradentate ligand between 1601 and 1465 cm^{-1} corresponding to the different $\nu_{C=C}$ and $\nu_{C=N}$ bond of these complexes (see Experimental section). In addition, the infrared spectra contained a strong band at around 841 cm^{-1} due to the ν_{P-F} bond of the counter ions for complexes **1** and **3** whereas for complex **2** it shows a strong band at around 661 cm^{-1} due to the ν_{Sb-F} bond of the counter ion.

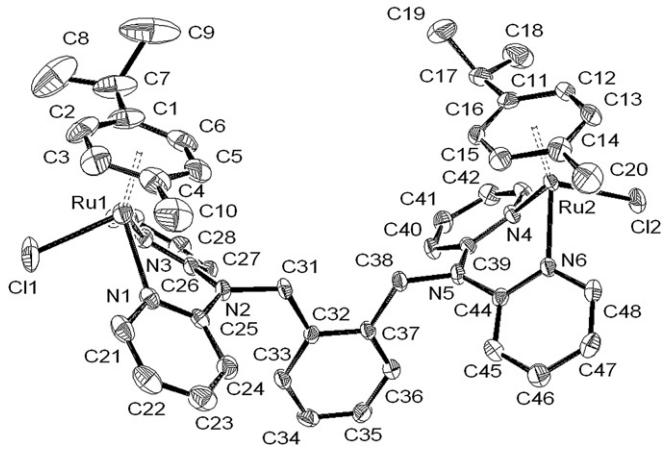

Fig. 1. Molecular structure of $[(\eta^6\text{-}p\text{-}^iPrC_6H_4Me)_2Ru_2(NN\cap NN)Cl_2](SbF_6)_2$ ([**2**]$(SbF_6)_2$) at 50% probability level. Hydrogen atoms and hexafluoroantimonate anions are omitted for clarity.

In the proton NMR spectra of **1**–**3**, the ligand signals shift to the downfield region as compared to that of the free ligand. The free ligand exhibits two doublets at around δ 8.32 and 7.25, two triplets at δ 7.56 and 6.88 corresponding to the different protons of the pyridyl groups. It also shows another doublet at δ 7.27 and a pseudo-triplet at δ 7.05 corresponding to the protons of the phenyl group of the ligand. In addition to this, a singlet is also observed at δ 5.52 which is due to the CH_2 protons of the ligand. However, after metallation, these peaks are shifted downfield in the range δ 9.01–5.77. In addition to the ligand signals mentioned in Experimental section, the ^{1}H NMR spectrum of complex **2** exhibit doublets at around δ 5.64 and 5.42 corresponding to the aromatic CH protons of the *p*-cymene ring. It also exhibits a singlet at δ 1.81, a doublet at δ 1.31 and a septet at δ 2.75 for the protons of the methyl and isopropyl groups of the *p*-cymene ligands. Interestingly the methyl group protons moved upfield compare to the starting dimer and also observed a single doublet for isopropyl protons instead of two doublets observed in other cases. However in the case of **1**, the proton NMR spectrum displays a singlet at δ 6.06 which corresponds to the protons of the benzene groups of the complex. The proton NMR spectrum of complex **3** exhibits a sharp singlet at δ 1.95 for the hexamethylbenzene ligand, which is shifted towards high field in comparison to the starting complex $[(\eta^6\text{-}C_6Me_6)Ru(\mu\text{-Cl})Cl]_2$ which shows at around δ 2.04. The molecular

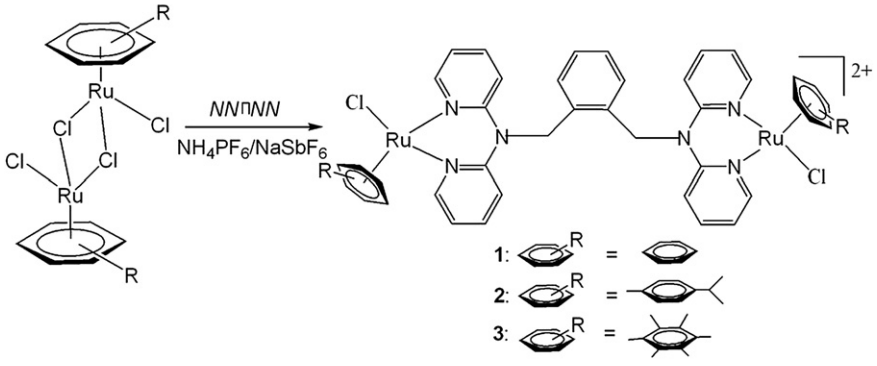

Scheme 1.

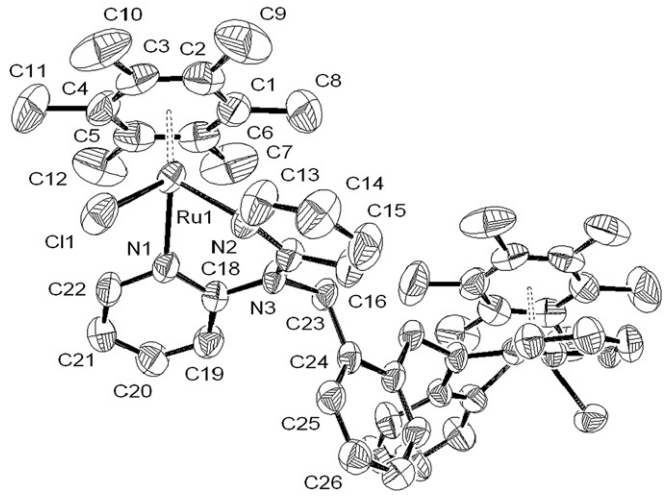

Fig. 2. Molecular structure of $[(\eta^6\text{-}C_6Me_6)_2Ru_2(NN\cap NN)Cl_2](PF_6)_2$ ($[\mathbf{3}](PF_6)_2\cdot H_2O.(CH_3)_2CO$) at 50% probability level. Hydrogen atoms, water, acetone and hexafluorophosphate anions are omitted for clarity. (Symmetry code: −x, y, ½ − z).

structures of the representative complexes **2** and **3** have been solved by single crystal X-ray diffraction study and the structures are presented in Figs. 1 and 2.

The reaction of the dimeric chloro complexes of $[(\eta^5\text{-}C_5Me_5)M(\mu\text{-}Cl)Cl]_2$ (M = Rh or Ir) with one equivalent of tetradentate ligand $NN\cap NN$ in methanol results in the formation of the yellow air stable dicationic dinuclear complexes $[(\eta^5\text{-}C_5Me_5)_2Rh_2(NN\cap NN)Cl_2]^{2+}$ (**4**) and $[(\eta^5\text{-}C_5Me_5)_2Ir_2(NN\cap NN)Cl_2]^{2+}$ (**5**) which are isolated as their hexafluorophosphate salts (Scheme 2). Complexes **4** and **5** are characterized by ^{1}H NMR, IR and mass spectroscopy. The infrared spectra of both the complexes exhibit sharp bands due to chelated $NN\cap NN$ tetradentate ligand and are given in Experimental section. Recently, we have reported a series of novel mono and binuclear complexes of platinum group metals with a similar type of $NN\cap NN$ tetradentate ligand 1,4-bis{bis(pyrazolyl-methyl)}benzene (see Chart 1) [29], where in the case of rhodium and iridium, we are able to synthesize both mono and binuclear complexes with the variation in metal to ligand ratio. But here in this case, only binuclear complexes are formed by the reaction of the metal complexes with the $NN\cap NN$ ligand, irrespective of the metal to ligand ratio. Several attempts to make mononuclear complexes by varying the metal complex ratio as well as changing different solvents were unsuccessful. The ^{1}H NMR spectra of these complexes show ligand peaks a downfield shift in the position of signals associated with protons of ligand $NN\cap NN$ compared to that of the uncoordinated ligand suggesting coordination of the nitrogen atoms to the metal center in a bidentate fashion. Beside the different proton peaks for the ligand as mentioned in Experimental section, the proton NMR spectra of these complexes exhibit a singlet at δ 1.59 and 1.56 corresponding to the protons of the pentamethylcyclopentadienyl group of these complexes.

The m/z values of all these complexes and their ion peaks obtained from the ESI mass spectra, as listed in Experimental section, which are in good agreement with the expected values. ESI mass spectra of the complexes displayed prominent peaks corresponding to the molecular ion fragment. These halogenated complexes displayed the prominent peak corresponding to the loss of chloride ion from the molecular ion peak, but the loss of Cp^* group is not observed indicating the stronger bond of metal to this group and remains intact. The molecular structure of representative compound **4** is solved by single crystal X-ray diffraction study and the structure is discussed later (Fig. 3).

*2.2. Dinuclear cyclopentadienyl ruthenium and osmium complexes **6**–**9***

Two equivalents of mononuclear cyclopentadienyl complexes $[(Cp)M(PPh_3)_2Cl]$ (M = Ru, Os; Cp = η^5-C_5H_5, η^5-C_9H_7, η^5-C_5Me_5) react with $NN\cap NN$ in refluxing methanol to give the corresponding dinuclear complexes **6**–**9** which are isolated as their hexafluorophosphate salts (Scheme 3). In this case also, our attempt to make mononuclear complexes with the variation of metal to ligand ratio was unsuccessful. The cationic complexes **6**–**9** are soluble in halogenated solvents and polar organic solvents such as tetrahydrofuran, methanol or dimethylsulfoxide but are insoluble in nonpolar solvents. All these complexes are stable in solid state as well as in solution. All complexes were characterized by IR, ^{1}H NMR, $^{31}P\{^1H\}$ NMR spectroscopy and mass spectrometry. The analytical data of these compounds are consistent with the formulations. Besides the IR bands as mentioned in Experimental section, these complexes also display a strong band between 842 and 846 cm^{-1} due to the ν_{P-F} stretching frequency of the counter ion of these complexes. The ^{1}H and $^{31}P\{^1H\}$ NMR spectra of complexes were recorded in $CDCl_3$ and spectral data are summarized in Experimental section. Shift in the position of signals associated with protons of ligand $NN\cap NN$, suggested coordination of nitrogen atom to the metal centre ruthenium and osmium in bidentate fashion. The protons of the ligand in these complexes **6**–**9** show a downfield shift with respect to the protons of the uncoordinated ligand. The ^{1}H NMR spectrum of the uncoordinated ligand displays peaks in between δ 8.26 and δ 5.52, whereas in the case of the metal complexes this peaks shifts to the downfield region at δ 9.37 and δ 5.54 respectively. In addition to the aromatic protons mentioned in Experimental section, complexes **6** and **7** show a singlet at δ 4.57 and δ 4.59 which corresponds to the cyclopentadienyl ring protons, indicating a downfield shift from the starting complexes. This downfield shift in the position of the cyclopentadienyl protons might result from a change in the electron density on the metal center due to the chelation of the $NN\cap NN$

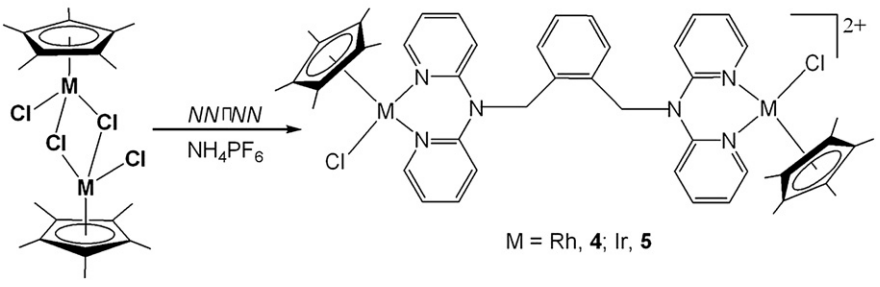

Scheme 2.

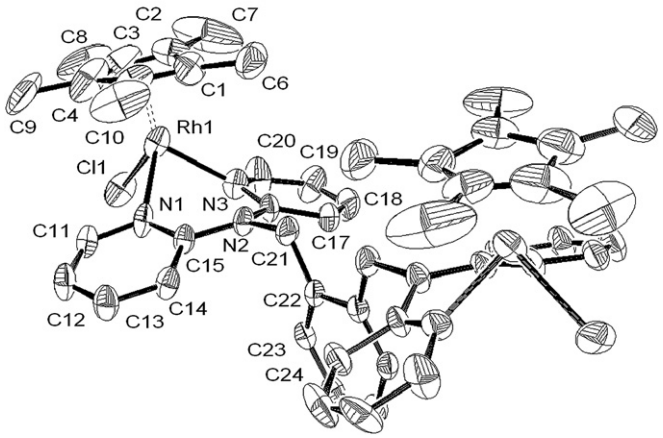

Fig. 3. Molecular structure of $[(\eta^6\text{-}C_5Me_5)_2Rh_2(NN\cap NN)Cl_2](PF_6)_2$ ([**4**]$(PF_6)_2$) at 25% probability level. Hydrogen atoms and hexafluorophosphate anions are omitted for clarity. (Symmetry code: −x, y, ½ − z).

ligand through nitrogen atoms. While in the case of complex **8** it displays a singlet at δ 2.04 corresponding to the methyl protons of the pentamethylcyclopentadienyl ligand. These complexes also show multiplets in the range of δ 7.66–7.21 due to the protons of the coordinated triphenylphosphine ligands. Complex **9** exhibits three sets of signals, triplet at δ 4.39, doublets at δ 4.95 and δ 4.80 corresponding to the protons of the indenyl group. The protons of the triphenylphosphine ligands exhibit a large multiplet centered at δ 7.33. In the $^{31}P\{^1H\}$ NMR spectra of the complexes **6**, **8** and **9**, the ^{31}P nuclei of the coordinated PPh_3 resonated as a sharp singlet in the range of δ 57.1–49.7 respectively whereas in the starting precursors the signal appears in the upfield region. In the case of complex **7** the $^{31}P\{^1H\}$ NMR spectrum displays a sharp singlet at δ −0.27 as compared to the starting complex which is found at δ −6.29. In addition to this, the $^{31}P\{^1H\}$ NMR spectrum of all these complexes shows a septet at δ −143 corresponding to the phosphorus atom present in the PF_6 counter ions. The *m*/*z* values of all these complexes and their stable ion peaks obtained from the ZQ mass spectra, as listed in Experimental section, are in good agreement with the theoretically expected values. ESI mass spectra of the complexes also displayed prominent peaks corresponding to the molecular ion fragment.

2.3. Molecular structures of [2](SbF6)2, [3](PF6)2.H2O.(CH3)2CO and [4](PF6)2

The complexes **3** and **4** crystallize in the space group *C*2/*c*, while complex **2** crystallizes in the space group $P2_1/n$. ORTEP drawings with the atom labeling scheme are shown in Fig. 1–3 and selected bond lengths and angles are presented in Table 1. The overall geometry of all these structures corresponds to the characteristic piano-stool configuration. All complexes contain two metal centers bonded to a η^5-C_5Me_5 or η^6-arene ligands, which are bridged by the tetradentate *NN*∩*NN* ligand through nitrogen atoms. The distance between the rhodium atom and the center of the η^5-C_5Me_5 ring is 1.759 Å in **4**, whereas the corresponding Ru–C_6Me_6 and Ru-*p*-cymene distances in **2** and **3** are shorter (1.687–1.697 Å). These bond lengths are comparable to those in related complexes [19–27]. The N–N and M-N bond distances in these complexes are comparable to each other, *i.e*., not much variation is observed. The M–Cl bond lengths are 2.3821(12) and 2.4028(11) in **2**, 2.3971(9) in **3** and 2.395(4) Å in **4**, which are closely similar to reported poly-pyridyl metal complexes [30,31].

In the crystal packing of [**3**]$(PF_6)_2\cdot H_2O\cdot(CH_3)_2CO$, the acetone molecule sits in the cavity of the dinuclear complex with the oxygen atom pointing down, see Fig. 4. The shortest C–H…O distances between the dinuclear complex **3** and the oxygen atom of the acetone molecule are respectively 2.444 Å with the C_6Me_6 ligand and 2.785 Å with the CH_2 groups. In addition to these interactions between the acetone molecule and the dinuclear complex, weak hydrogen bonds are observed between the water, the hexafluorophosphate anions and the complex.

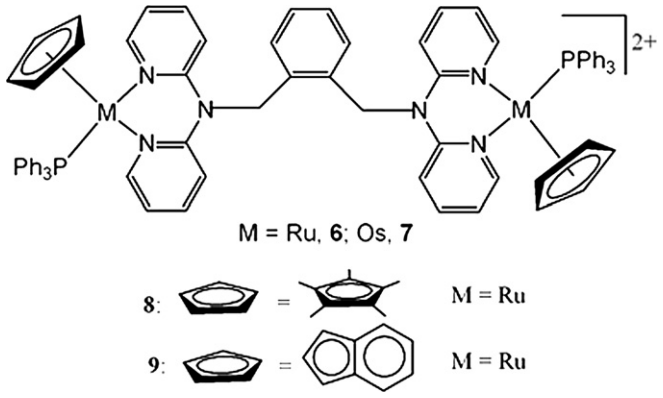

Scheme 3.

2.4. UV–vis spectroscopy

UV–vis spectra of the complexes **1**–**4**, **6** and **7** were acquired in acetonitrile and spectral data are summarized in Table 2. The low spin d^6 configuration of these dinuclear complexes provides filled orbitals of proper symmetry at the metal centers which can interact with the low lying π^* orbital of the ligands. One should therefore expect a band attributable to the metal to ligand charge transfer (MLCT) $t_{2g} \rightarrow \pi^*$ transition in their electronic spectra [32,33]. The electronic spectra of these complexes display a medium intensity band in the UV–vis region. The lowest energy absorption bands in the electronic spectra of these complexes in the visible region ~419–378 nm have been tentatively assigned on the basis of their intensity and position to $t_{2g} \rightarrow \pi^*$ MLCT transitions. The bands on the high energy side at ~305–232 nm for the complexes **1**–**4**, **6** and **7**, have been assigned to ligand-centered $\pi \rightarrow \pi^*$/n $\rightarrow \pi^*$ transitions [34,35]. In general, these complexes follow the normal trends observed in the electronic spectra of the nitrogen-bonded metal complexes, which display a ligand-based $\pi \rightarrow \pi^*$ transition for pyrazolyl pyridazine ligands in the UV region and metal to ligand charge transfer transitions in the visible region.

Table 1
Selected bond lengths and angles for complexes [**2**]$(SbF_6)_2$, [**3**]$(PF_6)_2.H_2O.(CH_3)_2CO$ and [**4**]$(PF_6)_2$.

	[**2**]$(SbF_6)_2$		[**3**]$(PF_6)_2$	[**4**]$(PF_6)_2$
	Ru(1)	Ru(2)	Ru(1)	Rh(1)
Inter atomic distances (Å)				
M–M	10.296(1)		11.654(1)[a]	11.580(3)[a]
M–N	2.091(4)	2.108(3)	2.091(3)	2.084(10)
M–N	2.091(4)	2.093(3)	2.097(3)	2.076(10)
M–Cl	2.3821(12)	2.4028(11)	2.397(9)	2.395(4)
M-centroid[b]	1.692	1.687	1.697	1.759
Angles (°)				
N–M–N	82.47(14)	80.76(13)	80.40(10)	81.0(4)
N–M–Cl	86.33(10)	87.44(9)	86.84(7)	89.4(3)
N–M–Cl	85.88(9)	88.02(9)	86.98(8)	88.5(3)

[a] symmetry code -x, y, ½-z;
[b] Calculated centroid-to-metal distances (η^6-C_6 or η^5-C_5 coordinated aromatic ring).

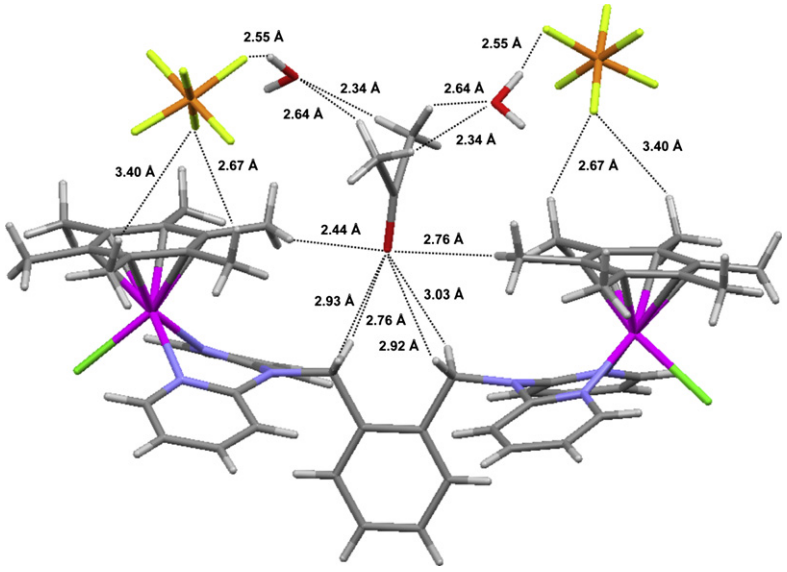

Fig. 4. Capped Sticks representation of [**3**]$(PF_6)_2.H_2O.(CH_3)_2CO$ showing the weak hydrogen-bonded network in the crystal.

3. Conclusions

In summary, here we described an easy and time saving procedure for the synthesis of the ligand 1, 2-bis(di-2-pyridylaminomethyl)benzene (*NN∩NN*) which has been previously reported, followed by the synthesis of nine dinuclear η^5- and η^6-cyclic hydrocarbon metal complexes bearing ligand *NN∩NN*, which are stable in the solid state and in solution have been successfully synthesized in good yield. The ligand has ability to form mononuclear, dinuclear and also tri- and tetra-nuclear complexes by variation of metal ligand ratio, however arene ruthenium and Cp^*Rh and Cp^*Ir reactions yielded dinuclear complexes only.

4. Experimental

4.1. Physical measurements

Infrared spectra were recorded on a Perkin–Elmer Model 983 spectrophotometer with the sample prepared as KBr pellets. The NMR spectra were obtained using Bruker Advance II 400 spectrometer in $CDCl_3$ for complexes using TMS as an internal standard. Mass spectra were obtained from a Waters ZQ - 4000 mass spectrometer by the ESI method. All chemicals used were of reagent grade. Elemental analyses of the complexes were performed on a Perkin–Elmer 2400 CHN/S analyzer. All reactions were carried out in distilled and dried solvents. The ligand *NN∩NN* was prepared by modification of a reported procedure [28] and is described below. The precursor complexes $[(\eta^6\text{-arene})Ru(\mu\text{-}Cl)Cl]_2$ (arene = C_6H_6, *p*-^{i}PrC_6H_4Me and C_6Me_6), $[(\eta^6\text{-}C_5Me_5)M(\mu\text{-}Cl)Cl]_2$ (M = Rh, Ir) [36–40], $[(\eta^5\text{-}C_5H_5)Ru(PPh_3)_2Cl]$, $[(\eta^5\text{-}C_5H_5)Os(PPh_3)_2Br]$, $[(\eta^5\text{-}C_5Me_5)Ru(PPh_3)_2Cl]$ and $[(\eta^5\text{-}C_9H_7)Ru(PPh_3)_2Cl]$ were prepared by following the literature methods [41–45].

Table 2
UV–vis absorption data in acetonitrile at 298 K.

Complex	λ_{max}/nm ($\epsilon/10^{-4}$ M^{-1} cm^{-1})			
1	232(0.65)	255(0.66)	299(0.49)	399(0.03)
2	233(0.61)	259(0.72)	304(0.57)	394(0.04)
3	235(0.99)	263(1.00)	305(0.94)	419(0.05)
4	233(0.68)		298(1.03)	397(0.06)
6	233(1.10)	261(0.96)		397(0.10)
7	249(0.58)		281(0.42)	378(0.05)

4.2. Single-crystal X-ray structures analyses

Crystals of complexes [**2**]$(SbF_6)_2$, [**3**]$(PF_6)_2\cdots H_2O\cdots(CH_3)_2CO$ and [**4**]$(PF_6)_2$ were mounted on a Stoe Image Plate Diffraction system equipped with a φ circle goniometer, using Mo-Kα graphite monochromated radiation (λ = 0.71073 Å) with range 0–200°. The structures were solved by direct methods using the program SHELXS-97 [46]. Refinement and all further calculations were carried out using SHELXL-97 [46]. The H-atoms were included in calculated positions and treated as riding atoms using the SHELXL default parameters. The non-H atoms were refined anisotropically, using weighted full-matrix least-square on F^2. Crystallographic details are summarized in Table 3 and selected bond lengths and angles are presented in Table 1. Fig. 1–3 were drawn with ORTEP-32 [47], while Fig. 4 was drawn with Mercury 2.3 [48].

4.3. Preparation of ligand 1,2-bis(di-2-pyridylaminomethyl) benzene (NN∩NN)

Di-2-pyridylamine (1.00 g, 5.84 mmol) and potassium hydroxide (1.33 g, 23.7 mmol) were stirred in DMSO (5 ml) for 1 h; 1,2-bis (bromomethyl)benzene (0.70 g, 2.65 mmol) was added and the reaction mixture was stirred for a further 4–5 h. The yellow precipitate that formed was isolated and purified by column chromatography (hexane/acetone 1:2) to give the desired product as a yellow solid which was recrystallized from acetone/diethylether to yield crystalline $C_{28}H_{24}N_6$. Yield, 0.31 g (26%); mp 144–147 °C. Found: C, 75.37; H, 5.38; N, 19.04. Calc. for $C_{28}H_{24}N_6$: C, 75.69; H, 5.52; N, 18.88%. ^{1}H NMR (400 MHz, $CDCl_3$): δ = 8.32 (d, 4H, py), 7.56 (t, 4H, py), 7.27 (d, 2H, ph), 7.22 (d, 4H, py), 7.06 (t, 2H, ph), 6.88 (dd, 4H, py), 5.63 (s, 4H, CH_2).

4.4. Preparation of $[(\eta^6\text{-arene})_2M_2(NN\cap NN)Cl_2](PF_6)_2$ {M = Ru, arene = C_6H_6 [1]$(PF_6)_2$, η^6-*p*-^{i}PrC_6H_4Me [**2**]$(SbF_6)_2$, C_6Me_6 [**3**]$(PF_6)_2$, M = Rh, arene = C_5Me_5 [**4**]$(PF_6)_2$ and M = Ir, arene = C_5Me_5 [**5**] $(PF_6)_2$ }

A mixture of $[(\eta^6\text{-arene})M(\mu\text{-}Cl)Cl]_2$ (M = Ru, Rh and Ir) (0.09 mmol), *NN∩NN* (40 mg, 0.09 mmol) and two equivalents of NH_4PF_6 ($NaSbF_6$ for complex **2**) was stirred in dry methanol (30 ml) for 4 h at room temperature. The yellow compound which formed was filtered, washed with ethanol, diethylether and dried under vacuum.

Table 3
Crystallographic and structure refinement parameters for complexes [**2**](SbF$_6$)$_2$, [**3**](PF$_6$)$_2$.H$_2$O.(CH$_3$)$_2$CO and ([**4**](PF$_6$)$_2$.

	[**2**](SbF$_6$)$_2$	[**3**](PF$_6$)$_2$.H$_2$O.acetone	[**4**](PF$_6$)$_2$
Chemical formula	$C_{48}H_{52}Cl_2F_{12}N_6Ru_2Sb_2$	$C_{55}H_{70}Cl_2F_{12}N_6O_3P_2Ru_2$	$C_{48}H_{54}Cl_2F_{12}N_6P_2Rh_2$
Formula weight	1457.50	1426.15	1281.63
Crystal system	Monoclinic	Monoclinic	Monoclinic
Space group	$P2_1/n$ (no. 14)	$C2/c$ (no. 15)	$C2/c$ (no. 15)
Crystal color and shape	Orange block	Orange block	Red block
Crystal size	0.23 × 0.21 × 0.19	0.22 × 0.19 × 0.18	0.22 × 0.20 × 0.17
a (Å)	12.4524(6)	26.655(2)	26.221(5)
b (Å)	35.6140(11)	13.7261(9)	13.460(3)
c (Å)	13.0152(6)	17.2504(13)	16.810(3)
β (°)	115.073(3)	110.207(6)	110.69(3)
V (Å^3)	5228.1(4)	5922.8(8)	5550.2(19)
Z	4	4	4
T (K)	203(2)	203(2)	173(2)
D_c (g cm^{-3})	1.852	1.599	1.534
μ (mm^{-1})	1.775	0.741	0.827
Scan range (°)	$1.82 < \theta < 29.22$	$1.63 < \theta < 28.35$	$2.33 < \theta < 26.01$
Unique reflections	14115	7046	5093
Reflections used [$I > 2\sigma(I)$]	9942	5288	2735
R_{int}	0.0769	0.0529	0.0542
Final R indices [$I > 2\sigma(I)$][a]	0.0496, wR_2 0.00954	0.0463, wR_2 0.1404	0.1061, $wR_2$0.3151
R indices (all data)	0.0841, wR_2 0.1052	0.0620, wR_2 0.1519	0.1500, $wR_2$0.3341
Goodness-of-fit	1.020	1.057	1.099
Max, Min $\Delta\rho$/e (Å^{-3})	0.947, −1.504	1.029, −0.710	1.543, −0.968

[a] Structures were refined on F_0^2: $wR_2 = [\Sigma[w(F_0^2 - F_c^2)^2]/\Sigma w(F_0^2)^2]^{1/2}$, where $w^{-1} = [\Sigma(F_0^2) + (aP)^2 + bP]$ and $P = [\max(F_0^2, 0) + 2F_c^2]/3$.

4.4.1. Compound [**1**](PF$_6$)$_2$

Yield: 145 mg, 74.7%. Elemental Anal (%) Calc. for $C_{40}H_{36}Cl_2F_{12}N_6P_2Ru_2$: C 41.29; H 3.13; N 7.21; found: C 41.58; H 3.55; N 6.92; IR (KBr pellets, cm^{-1}): 1601 ($\nu_{C=C}$); 1466 ($\nu_{C=N}$); 843 (ν_{P-F}); ^{1}H NMR (400 MHz, CDCl$_3$): δ = 9.01 (dd, 4H, Py), 8.05 (dt, 4H, Py), 7.51 (d, 2H, Ph), 7.47−7.43 (m, 6H, Py and Ph), 7.41 (t, 4H, Py), 6.06 (s, 12H, C_6H_6), 5.83 (s, 4H, CH_2); ESI-MS (m/z): 871.3 [M-(PF$_6$)$_2$]$^+$, 800.3 [M-(PF$_6$)$_2$-Cl$_2$]$^+$.

4.4.2. Compound [**2**](SbF$_6$)$_2$

Yield: 136 mg, 73%. Elemental Anal (%) Calc. for $C_{38}H_{38}Cl_2F_{12}N_6Sb_2Ru_2$: C 39.99; H 3.37; N 7.35; found: C 40.44; H 3.66; N 7.15. IR (KBr pellets, cm^{-1}): 1600 ($\nu_{C=C}$); 1467 ($\nu_{C=N}$); 661 (ν_{Sb-F}); ^{1}H NMR (400 MHz, CDCl$_3$): δ = 8.68 (d, 4H, Py), 7.89 (dt, 4H, Py), 7.38 (d, 2H, Ph), 7.34 (d, 4H, Py), 7.25 (t, 2H, Ph), 7.15 (t, 4H, Py), 5.77 (s, 4H, CH_2), 5.64 (d, 4H, Ar_{p-cy}), 5.42 (d, 4H, Ar_{p-cy}), 2.75 (sept. 2H), 1.81 (s, 6H), 1.31 (d, 12H).

4.4.3. Compound [**3**](PF$_6$)$_2$

Yield: 143 mg, 71.8%. Elemental Anal (%) Calc. for $C_{52}H_{60}Cl_2F_{12}N_6P_2Ru_2$: C 46.87; H 4.57; N 6.30; found: C 47.08; H 4.89; N 6.04. IR (KBr pellets, cm^{-1}): 1597 ($\nu_{C=C}$); 1465 ($\nu_{C=N}$); 843 (ν_{P-F}); ^{1}H NMR (400 MHz, CDCl$_3$): δ = 8.52 (dd, 4H, Py), 7.89 (dt, 4H, Py), 7.35 (d, 2H, Ph), 7.28 (t, 4H, Py), 7.22 (t, 2H, Ph), 6.92 (t, 4H, Py), 5.77 (s, 4H, CH_2), 1.95 (s, 36H, C_6Me_6); ESI-MS (m/z): 1042.4 [M-(PF$_6$)$_2$]$^+$, 971.4 [M-(PF$_6$)$_2$-Cl$_2$]$^+$.

4.4.4. Compound [**4**](PF$_6$)$_2$

Yield: 159 mg, 76.8%. Elemental Anal (%) Calc. for $C_{48}H_{54}Cl_2F_{12}N_6P_2Rh_2$: C 45.01; H 4.27; N 6.55; found: C 45.37; H 4.49; N 6.23. IR (KBr pellets, cm^{-1}): 1616 ($\nu_{C=C}$); 1445 ($\nu_{C=N}$); 842 (ν_{P-F}); ^{1}H NMR (400 MHz, CDCl$_3$): δ = 8.68 (dd, 4H, Py), 7.93 (dt, 4H, Py), 7.41 (d, 2H, Ph), 7.38 (t, 4H, Py), 7.33−7.21 (m, 6H, Py and Ph), 5.78 (s, 4H, CH_2), 1.59 (s, 30H, C_5Me_5); ESI-MS (m/z): 991.5 [M-(PF$_6$)$_2$]$^+$, 920.4 [M-(PF$_6$)$_2$-Cl$_2$]$^+$.

4.4.5. Compound [**5**](PF$_6$)$_2$

Yield: 109 mg, 72.2%. Elemental Anal (%) Calc. for $C_{48}H_{54}Cl_2F_{12}N_6P_2Ir_2$: C 39.48; H 3.75; N 5.75; found: C 40.05; H 3.97; N 5.43. IR (KBr pellets, cm^{-1}): 1622 ($\nu_{C=C}$); 1415 ($\nu_{C=N}$); 842 (ν_{P-F}); ^{1}H NMR (400 MHz, CDCl$_3$): δ = 8.74 (dd, 4H, Py), 8.01 (dt, 4H, Py), 7.61 (d, 2H, Ph), 7.41 (t, 4H, Py), 7.39−7.23 (m, 6H, Py and Ph), 5.83 (s, 4H, CH_2), 1.56 (s, 30H, C_5Me_5); ESI-MS (m/z): 1169.8 [M-(PF$_6$)$_2$]$^+$, 1098.4 [M-(PF$_6$)$_2$-Cl$_2$]$^+$.

4.5. Preparation of [(η^5-Cp)$_2$M$_2$(NN∩NN)(PPh$_3$)$_2$](PF$_6$)$_2$ {Cp = C$_5$H$_5$, M = Ru [**6**](PF$_6$)$_2$, Os [**7**](PF$_6$)$_2$, Cp = C$_5$Me$_5$, M = Ru [**8**](PF$_6$)$_2$ and Cp = C$_9$H$_7$, M = Ru [**9**](PF$_6$)$_2$}

A mixture of [(η^5-Cp)M(PPh$_3$)$_2$X] {M = Ru, X = Cl and M = Os, X = Br} (0.18 mmol), *NN∩NN* (40 mg, 0.09 mmol) and two equivalents of NH_4PF_6 in dry methanol (30 ml) were refluxed for 12 h until the color of the solution changed from pale yellow to orange. The solvent was removed under vacuum, the residue was dissolved in dichloromethane (10 ml), and the solution filtered to remove ammonium halide. The orange solution was concentrated to 5 ml, upon addition of diethylether the orange−yellow complex was precipitated, which was separated and dried under vacuum.

4.5.1. Compound [**6**](PF$_6$)$_2$

Yield: 163 mg, 74.4%. Elemental Anal (%) Calc. for $C_{74}H_{64}F_{12}N_6P_4Ru_2$: C 55.86; H 4.06; N 5.26; found: C 56.11; H 4.37; N 5.02. IR (KBr pellets, cm^{-1}): 1596 ($\nu_{C=C}$); 1436 ($\nu_{C=N}$); 842 (ν_{P-F}); ^{1}H NMR (400 MHz, CDCl$_3$): δ = 8.59 (dd, 4H, Py), 7.93 (dt, 4H, Py), 7.55 (d, 2H, Ph), 7.33−7.21 (m, 30H, PPh_3), 7.18 (t, 4H, Py), 7.12 (t, 2H, Ph), 6.87 (t, 4H, Py), 5.73 (s, 4H, CH_2), 4.57 (s, 10H, C_5H_5); ESI-MS (m/z): 1301.1 [M-(PF$_6$)$_2$]$^+$; ^{31}P{^{1}H} NMR (CDCl$_3$, δ): 50.85 (s, PPh_3), −143 (sept, PF_6).

4.5.2. Compound [**7**](PF6)2

Yield: 160 mg, 75.1%. Elemental Anal (%) Calc. for $C_{74}H_{64}F_{12}N_6P_4Os_2$: C 50.24; H 3.65; N 4.74; found: C 50.59; H 3.92; N 4.56. IR (KBr pellets, cm^{-1}): 1615 ($\nu_{C=C}$); 1465 ($\nu_{C=N}$); 842 (ν_{P-F}); ^{1}H NMR (400 MHz, CDCl$_3$): δ = 8.66 (dd, 4H, Py), 7.97 (dt, 4H, Py), 7.53 (d, 2H, Ph), 7.39−7.26 (m, 30H, PPh_3), 7.15 (t, 4H, Py), 7.07 (t, 2H, Ph), 6.65 (t, 4H, Py), 5.66 (s, 4H, CH_2), 4.59 (s, 10H, C_5H_5); ESI-MS (m/z): 1479.1 [M-(PF$_6$)$_2$]$^+$; ^{31}P{^{1}H} NMR (CDCl$_3$, δ): −0.27 (s, PPh_3), −143 (sept, PF_6).

*4.5.3. Compound [**8**](PF$_6$)$_2$*

Yield: 161 mg, 74.2%. Elemental Anal (%) Calc. for $C_{84}H_{84}F_{12}N_6P_4Ru_2$: C 58.27; H 4.89; N 4.83; found: C 58.63; H 5.19; N 4.59. IR (KBr pellets, cm^{-1}): 1642 ($\nu_{C=C}$); 1401 ($\nu_{C=N}$); 844 (ν_{P-F}); ^{1}H NMR (400 MHz, $CDCl_3$): $\delta = 9.32$ (dd, 4H, Py), 8.65 (dt, 4H, Py), 8.32 (d, 2H, Ph), 7.66–7.49 (m, 30H, PPh_3), 7.38 (t, 4H, Py), 7.31 (t, 2H, Ph), 6.98 (t, 4H, Py), 5.63 (s, 4H, CH_2), 2.04 (s, 30H, C_5Me_5). ESI-MS (m/z): 1441.2 [M-(PF$_6$)$_2$]$^+$; ^{31}P{^{1}H} NMR ($CDCl_3$, δ): 49.7 (s, PPh_3), −143 (sept, PF_6).

*4.5.4. Compound [**9**](PF$_6$)$_2$*

Yield: 163 mg, 76.8%. Elemental Anal (%) Calc. for $C_{82}H_{68}F_{12}N_6P_4Ru_2$: C 58.24; H 4.07; N 4.95; found: C 58.59; H 4.40; N 5.27. IR (KBr pellets, cm^{-1}): 1616 ($\nu_{C=C}$); 1415 ($\nu_{C=N}$); 846; ^{1}H NMR (400 MHz, $CDCl_3$): $\delta = 9.37$ (dd, 4H, Py), 8.72 (dt, 4H, Py), 8.31 (d, 2H, Ph), 7.65–7.20 (m, 38H, PPh_3 and indenyl), 7.07 (t, 4H, Py), 6.97 (t, 2H, Ph), 6.81 (t, 4H, Py), 5.54 (s, 4H, CH_2), 4.95 (d, 2H, indenyl), 4.80 (d, 2H, indenyl), 4.39 (t, 2H, indenyl). ESI-MS (m/z): 1401.1 [M- (PF$_6$)$_2$]$^+$; ^{31}P{^{1}H} NMR ($CDCl_3$, δ): 57.10 (s, PPh_3), −143 (sept, PF_6).

Appendix A. Supplementary material

CCDC-790563 ([**2**](SbF$_6$)$_2$), 790564 ([**3**](PF$_6$)$_2$···H$_2$O···(CH$_3$)$_2$CO) and 790565 ([**4**](PF$_6$)$_2$) contain the supplementary crystallographic data for this paper. These data can be obtained free of charge via www.ccdc.cam.ac.uk/data_request/cif.

References

[1] P. Gamez, P. de Hoog, O. Roubeau, M. Lutz, W.L. Driessen, A.L. Spek, J. Reedijk, Chem. Commun. (2002) 1488–1489.
[2] W.-L. Jia, D.-R. Bai, T. McCormick, Q.-D. Liu, M. Motala, R.-Y. Wang, C. Seward, Y. Tao, S. Wang, Chem. Eur. J. 10 (2004) 994–1006.
[3] C. Seward, J. Pang, S. Wang, Eur. J. Inorg. Chem. (2002) 1390–1399.
[4] Y. Kang, C. Seward, D. Song, S. Wang, Inorg. Chem. 42 (2003) 2789–2797.
[5] C. Seward, W.-L. Jia, R.-Y. Wang, G.D. Enright, S. Wang, Angew. Chem., Int. Ed. Engl. 43 (2004) 2933–2936.
[6] J.E. Johnson, T.A. Beinke, R.A. Jacobson, J. Chem. Soc. A (1971) 1371–1374.
[7] J. Sletten, K. Svardal, A. Sorensen, Acta. Chem. Scand. 47 (1993) 1091–1099.
[8] W.L. Johnson, J.F. Geldard, Inorg. Chem. 18 (1979) 664–669.
[9] C. Tu, J. Lin, Y. Shao, Z. Guo, Inorg. Chem. 42 (2003) 5795–5797.
[10] T. Chao, Y. Shao, N. Gan, Q. Xu, Z. Guo, Inorg. Chem. 43 (2004) 4761–4766.
[11] D.P. Segers, Ph.D. Thesis, North Carolina State University.
[12] Y. Wang, Y. Mizubayashi, M. Odoko, N. Okabe, Acta Crystallogr. C 61 (2005) m67–m70.
[13] I. Puscasu, C. Mock, M. Rauterkus, A. Rondigs, G. Tallen, S. Gangopadhyay, J.E.A. Wolff, B. Krebs, Z. Anorg. Allg. Chem. 627 (2001) 1292–1298.
[14] S. Fakih, W.C. Tung, D. Eierhoff, C. Mock, B. Krebs, Z. Anorg. Allg. Chem. 631 (2005) 1397–1402.
[15] P. Štěpnička, J. Ludvík, J. Canivet, G. Süss-Fink, Inorg. Chim. Acta 359 (2006) 2369–2374 and references therein.
[16] B. Therrien, Coord. Chem. Rev. 253 (2008) 493–519.
[17] E. Wong, C.M. Giandomenico, Chem. Rev. 99 (1999) 2451–2466.
[18] R.H. Crabtree, The Organometallic Chemistry of the Transition Metals, fourth ed.. John Wiley and Sons, Hoboken, NJ, 2005.
[19] G. Gupta, G.P.A. Yap, B. Therrien, K. Mohan Rao, Polyhedron 28 (2009) 844–850.
[20] K.S. Singh, Y.A. Mozharivskyj, P.J. Carroll, K. Mohan Rao, J. Organomet. Chem. 689 (2004) 1249–1256.
[21] G. Gupta, K.T. Prasad, B. Das, G.P.A. Yap, K. Mohan Rao, J. Organomet. Chem. 694 (2009) 2618–2627.
[22] G. Gupta, B. Therrien, K. Mohan Rao, J. Organomet. Chem. 695 (2010) 753–759.
[23] G. Gupta, K.T. Prasad, B. Das, K. Mohan Rao, Polyhedron 29 (2010) 904–910.
[24] G. Gupta, C. Zheng, P. Wang, K. Mohan Rao, Z. Anorg. Allg. Chem. 636 (2010) 758–764.
[25] K.T. Prasad, G. Gupta, M.P. Pavan, A.K. Chandra, K. Mohan Rao, J. Organomet. Chem. 695 (2010) 707–716.
[26] G. Gupta, K.T. Prasad, A.V. Rao, S.J. Geib, B. Das, K. Mohan Rao, Inorg. Chim. Acta 363 (2010) 2287–2295.
[27] G. Gupta, S. Gloria, B. Das, K. Mohan Rao, J. Mol. Struct. 979 (2010) 205–213.
[28] B. Antonioli, D.J. Bray, J.K. Clegg, K. Gloe, K. Gloe, O. Kataeva, L.F. Lindoy, J.C. Mc Murtrie, P.J. Steel, C.J. Sumby, M. Wenzel, J. Chem. Soc. Dalton Trans. (2006) 4783–4794.
[29] K.T. Prasad, B. Therrien, K. Mohan Rao, J. Org. Chem. 695 (2010) 1375–1382.
[30] B. Therrien, C.S. -Mohamed, G. Süss-Fink, Inorg. Chim. Acta 361 (2008) 2601–2608.
[31] P. Govindaswamy, J. Canivet, B. Therrien, G. Süss-Fink, P. Štěpnička, J. Ludvík, J. Organomet. Chem. 692 (2007) 3664–3675.
[32] A.B.P. Lever, Inorganic Electronic Spectroscopy. Elsevier, Amsterdam, 1968.
[33] M. Gerloch, E.C. Constable, Transition Metal Chemistry: The Valence Shell in d-Block Chemistry. VCH, 1994.
[34] P. Didier, I. Ortmans, A.K.D. Mesmacker, R.J. Watts, Inorg. Chem. 32 (1993) 5239–5245.
[35] B.P. Sulliran, D.J. Salmon, T.J. Meyer, Inorg. Chem. 17 (1978) 3334–3341.
[36] M.A. Bennett, T.N. Huang, T.W. Matheson, A.K. Smith, Inorg. Synth. 21 (1982) 74–78.
[37] M.A. Bennett, T.W. Matheson, G.B. Robertson, A.K. Smith, P.A. Tucker, Inorg. Chem. 19 (1980) 1014–1021.
[38] M.A. Bennett, A.K. Smith, J. Chem. Soc. Dalton Trans. (1974) 233–241.
[39] J.W. Kang, K. Moseley, P.M. Maitlis, J. Am. Chem. Soc. 91 (1969) 5970–5977.
[40] C. White, A. Yates, P.M. Maitlis, Inorg. Synth. 29 (1992) 228–230.
[41] M.I. Bruce, C. Hameister, A.G. Swincer, R.C. Wallis, Inorg. Synth. 28 (1990) 270–272.
[42] P.W. Wanandi, T.D. Tilley, Organometallics 16 (1997) 4299–4313.
[43] M.I. Bruce, P.J. Low, B.W. Skelton, E.R.T. Tiekink, A. Werth, A.H. White, Aust. J. Chem. 48 (1995) 1887–1892.
[44] M.I. Bruce, B.C. Hall, N.N. Zaitseva, B.W. Skelton, A.H. White, J. Chem. Soc. Dalton Trans. (1998) 1793–1804.
[45] L.A. Oro, M.A. Ciriano, M. Campo, C. Foces-Foces, F.H. Cano, J. Organomet. Chem. 289 (1995) 117–131.
[46] G.M. Sheldrick, Acta. Crystallogr. A64 (2008) 112–122.
[47] L.J. Farrugia, J. Appl. Cryst. 30 (1997) 565–566.
[48] I.J. Bruno, J.C. Cole, P.R. Edgington, M. Kessler, C.F. Macrae, P. McCabe, J. Pearson, R. Taylor, Acta Crystallogr. B58 (2002) 389–397.